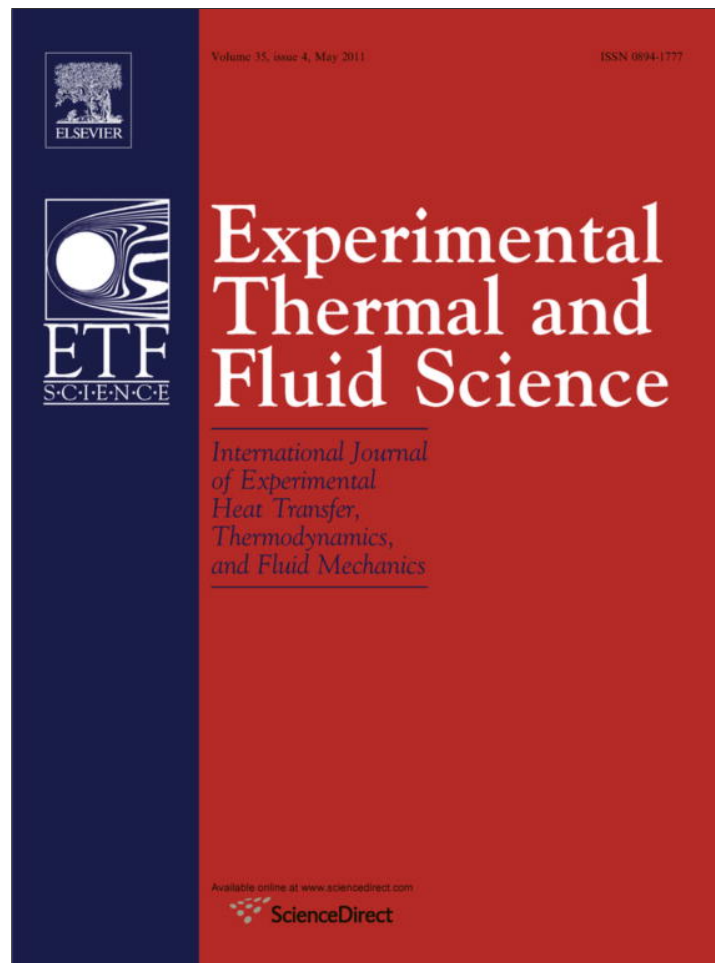


Provided for non-commercial research and education use.
Not for reproduction, distribution or commercial use.



This article appeared in a journal published by Elsevier. The attached copy is furnished to the author for internal non-commercial research and education use, including for instruction at the authors institution and sharing with colleagues.

Other uses, including reproduction and distribution, or selling or licensing copies, or posting to personal, institutional or third party websites are prohibited.

In most cases authors are permitted to post their version of the article (e.g. in Word or Tex form) to their personal website or institutional repository. Authors requiring further information regarding Elsevier's archiving and manuscript policies are encouraged to visit:

<http://www.elsevier.com/copyright>



Contents lists available at ScienceDirect

Experimental Thermal and Fluid Science

journal homepage: www.elsevier.com/locate/etfs

Analysis of energy consumption in microwave and convective drying process of multi-layered porous material inside a rectangular wave guide

W. Jindarat, P. Rattanadecho*, S. Vongpradubchai

Research Center of Microwave Utilization in Engineering (RCME), Department of Mechanical Engineering, Faculty of Engineering, Thammasat University (Rangsit Campus), Pathumthani 12120, Thailand

ARTICLE INFO

Article history:

Received 30 September 2009
Received in revised form 5 August 2010
Accepted 24 November 2010
Available online 28 November 2010

Keywords:

Microwave energy
Drying process
Multi-layered porous material
Specific energy consumption (SEC)
Energy efficiency

ABSTRACT

This work applies the first law of thermodynamics to estimate the ratio of energy utilization in microwave drying process using a rectangular waveguide. Two porous packed bed systems are considered such as attaching fine bed on coarse bed (F–C) and attaching coarse bed on fine bed (C–F). The effects of layered configuration and layered thickness on drying rate, power absorbed efficiency, specific energy consumption (SEC), and energy efficiency are studied in detail. The results show that the variations of all parameters have strongly affected on microwave penetration depth and power absorbed within the packed bed. Furthermore, F–C bed with equal layer thickness corresponds to great energy efficiency.

© 2010 Elsevier Inc. All rights reserved.

1. Introduction

Energy used in the drying and heating process is important for production processes in the industrial and household sectors. However, the price of energy is extremely expensive; therefore, there are a strong incentive to invent processes that will use energy efficiently. Currently, widely used drying and heating processes are complicated and inefficient; moreover, it is generally damaging to the environment. What is needed is a simplified, lower-cost approach to this process one that will be replicable in a range of situations.

The conventional drying process had been a central subject for research and development was investigated by Maroulis et al. [1] where a study of drying parameter to apply the design for conveyor belt drying has carried out: a study by Men'Shutina et al. [2] focused on thermal efficiency in the conveyor belt dryer process, and Akpınar [3] analyzed the energy and exergy in red of pepper slices drying with a convective-type dryer.

For an analysis of energy consumption during applied microwave energy on heating and drying processes has been investigated by many researches. Sharma and Prasad [4], this study examined the specific energy consumption in microwave drying

of garlic cloves. The drying processes used to microwave and hot air drying in accordance with microwave oven for comparing specific energy consumption (SEC). Other important papers [1–13] were addressing the combined microwave energy and hot air drying processes for several kinds of dielectric materials. Such as Varith et al. [5], was studying of the combined microwave and hot air drying of peeled longan, which investigated the variation of moisture content and SEC in several drying conditions. Another important studied, Lakshmi et al. [6], was comparison the variation of SEC in cooking rice among the microwave oven, electric rice cooker and pressure cooker.

For theoretical research, Rattanadecho et al. [7] studied the influence of irradiation time, particle size, and initial moisture content on drying kinetics during microwave drying of multi-layered capillary porous materials in a rectangular waveguide. Feng et al. [8] carried out combined microwave and spouted bed drying process for diced apple. Experimental results of heat and mass transport were the compared to the results from a mathematical model.

From the previous works, the effects of sample structure and the SEC were minimal studied in drying processes. The objective of this study is to experimentally analyze the effects of layered configuration and layered thickness on the microwave drying of multi-layered porous packed bed with a rectangular waveguide. An operating frequency is 2.45 GHz. The knowledge gained will provide an understanding in porous media and the parameters which can help to reduce the SEC.

* Corresponding author. Tel.: +66 02 564 3001 9, fax: +66 02 564 3010.
E-mail address: ratphadu@engr.tu.ac.th (P. Rattanadecho).

Nomenclature

A	porous packed bed surface area (m^2)	X	absolute humidity (kg_{vapor}/kg_{dryair})
C_p	specific heat of the dielectric material ($kJ/kg\ K$)	<i>Greek letters</i>	
c_m	material specific heat ($kJ/kg\ K$)	ϵ_r''	relative dielectric loss factor
D_p	penetration depth (m)	ϵ_r'	relative dielectric constant
d_p	dept of packed bed (mm)	ϵ_0	permittivity of air (F/m)
E	electromagnetic field intensity (V/cm)	X	humidity ratio (kg_{vapor}/kg_{dryair})
f	microwave frequency (Hz)	ΔT	the increment temperature ($^{\circ}C$)
h	enthalpy (kJ/kg)	η_{abs}	microwave power absorbed efficiency (%)
h_m	enthalpy of material (kJ/kg)	η_e	energy efficiency (%)
\bar{h}	convection heat transfer coefficient ($W/m^2\ K$)	ρ_s	density of solid (glass bead) (kg/m^3)
h_{fg}	latent heat of vaporization (kJ/kg_{water})	ρ_w	density of water (kg/m^3)
k	thermal conductivity ($W/m\ K$)	ϕ	porosity (m^3/m^3)
M_p	particle moisture content dry basis (kg_{water}/kg_{solid})	v	velocity of propagation (m/s)
\dot{m}	mass flow rate (kg/s)	ρ	density (kg/m^3)
\dot{m}_a	mass flow rate of dry air (kg/s)	ω	angular velocity of microwave (rad/s)
\dot{m}_w	mass flow rate of water from the surface of a porous packed bed (kg/s)	<i>Subscripts</i>	
\bar{N}_{tu}	Nusselt number	o	standard state value
P_{in}	microwave power incident (microwave energy emitted from a microwave oscillator) (kW)	0	free space
P_1	density of microwave power absorbed by dielectric material (kW/cm^3)	1	inlet
P_2	energy is required to heat up the dielectric material (kW)	2	outlet
P_{abs}	microwave power absorbed (kW)	a	air
P_{tran}	microwave power transmitted (kW)	ab	absorb
P_{ref}	microwave power reflected (kW)	b	before
Q_{evap}	heat transfer rate due to water evaporation (kW)	$convec$	convection
Q_{abs}	microwave energy to be required for heating up dielectric material (kW)	da	drying air
\dot{Q}_{loss}	heat transfer rate to the environment (kW)	d	dry material
Q_{convec}	convection heat transfer (kW)	fg	difference in property between saturated liquid and saturated vapor
SEC	specific energy consumption (kJ/kg)	g	gas
S	water saturation	in	input
T	temperature ($^{\circ}C$)	l	liquid water
T_{surf}	temperature at porous packed bed surface ($^{\circ}C$)	m	material
T_{∞}	ambient temperature ($^{\circ}C$)	out	output
t	time (s)	ref	reflect
$\tan \delta$	loss tangent coefficient (-)	r	relative
W	weight of the dielectric material (kg)	s	solid
W_d	weight of dry material (kg)	$surf$	surface
W_b	weight of material before drying (kg)	$tran$	transmit
W_{in}	total work entering the system (kJ)	v	vapor
W_{out}	total work leaving the system (kJ)	w	water
		∞	ambient condition

2. Experimental apparatus

Fig. 1 shows the experimental apparatus of microwave drying of the porous packed bed using a rectangular waveguide. The microwave system was a monochromatic wave of TE_{10} mode operating at a frequency of 2.45 GHz. Microwave energy was generated by magnetron (Micro Denshi Co., model UM-1500, Tokyo, Japan); it was transmitted along the z-direction of the rectangular waveguide with inside dimensions of 110 mm \times 55 mm toward a water load situated at the end of the waveguide. The water load (lower absorbing boundary) ensured that only a minimal amount of microwave energy was reflected back to the sample. In addition, an isolator (upper absorbing boundary) was used to trap any microwave energy reflected from the sample to prevent it from damaging the magnetron. The output of the magnetron was adjustable from 0 to 1500 W. The power of incident, reflected and transmitted waves were measured by a wattmeter using a directional coupler (Micro Denshi Co., model DR-5000, Tokyo, Japan). The

distributions of temperature within the porous packed bed were measured using fiberoptic (LUXTRON Fluoroptic Thermometer, Model 790, Santa Clara, Canada, accurate to $\pm 0.5^{\circ}C$). The fiberoptic probes were inserted into the sample at the center and at the following depth from the surface of the packed bed: 5, 15, 25, and 35 mm (as seen in Fig. 2).

As seen in Fig. 3, the samples were porous packed bed, which composed of glass beads, water, and air. A sample container was made from polypropylene with a thickness of 1 mm, it did not absorb microwave energy. In this study, the voids occupy from a fraction up to 38 percent of the whole volume of packed beds. The dimensions of packed bed are chosen to be 110 mm \times 50 mm. The samples were prepared in two configurations: a single-layered packed bed (fine bed with diameter of 0.15 mm (F-bed) and coarse bed with diameter of 0.40 mm (C-bed)) and two-layered packed bed, respectively. The case of two-layered packed bed was classified in two configurations: F-C bed (attaching fine bed ($d = 0.15$ mm, $d_p = 10, 20, 25, 30,$ and 40 mm) on coarse bed

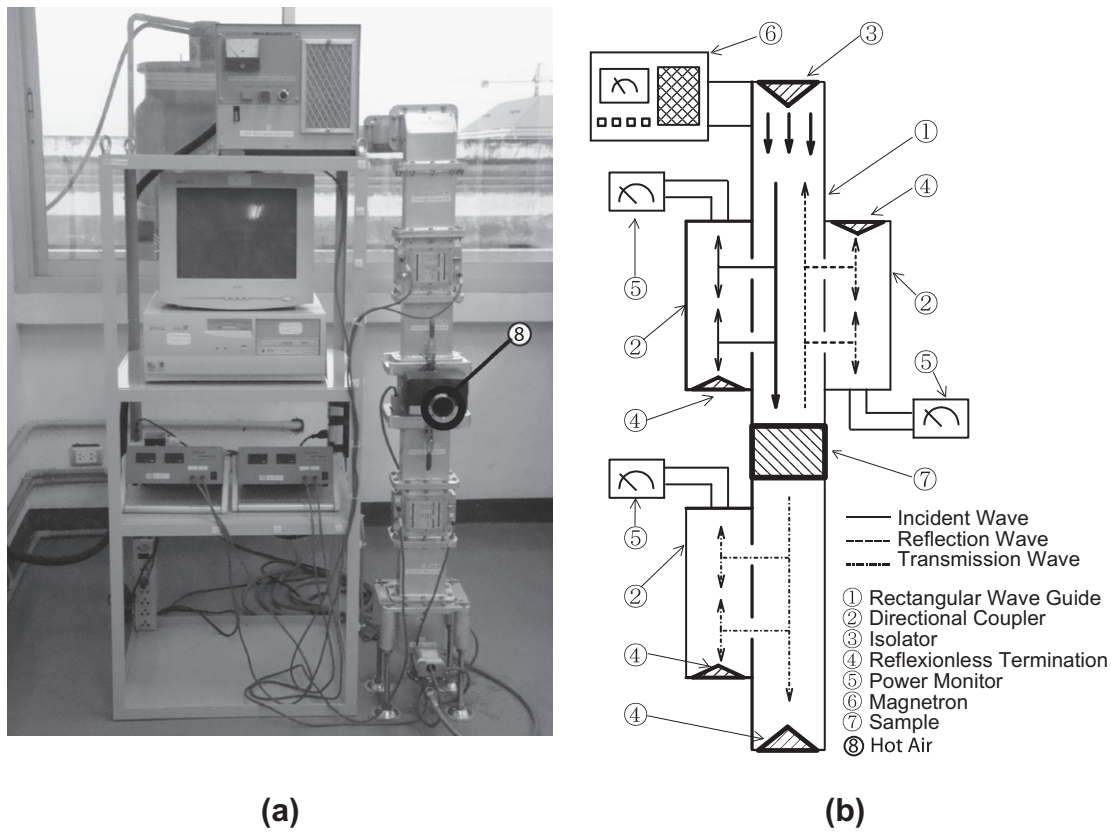


Fig. 1. Schematic of experimental facility: (a) equipment setup; (b) microwave measuring system.

($d = 0.40$ mm, $d_p = 40, 30, 25, 20,$ and 10 mm) and C–F bed (attaching coarse bed ($d = 0.40$ mm, $d_p = 10, 20, 25, 30,$ and 40 mm) on fine bed ($d = 0.15$ mm, $d_p = 40, 30, 25, 20,$ and 10 mm), respectively. The water saturations in the packed bed were defined as the fraction of the volume occupied by water to volume of the pores. They were obtained by weighing dry and wet mass of the sample which were cut out in volume (four positions) of about 110 mm \times

354.61 mm \times 312.5 mm at the end of each run. The water saturation formula can be described in the following from [7]:

$$S = \frac{M_p \cdot \rho_s \cdot (1 - \phi)}{\rho_w \cdot \phi \cdot 100} \quad (1)$$

where S is water saturation; ρ_s is density of solid; ρ_w is density of water; ϕ is porosity and M_p is particle moisture content dry basis. During the experimental microwave drying processes, the uncertainty of our data might come from the variations in humidity and room temperature. The uncertainty in drying kinetics was assumed to result from errors in the measured weight of the sample. The calculated drying kinetic uncertainties in all tests were less than 3%. The uncertainty in temperature was assumed to result from errors in measured input power, ambient temperature and ambient humidity. The calculated uncertainty associated with temperature was less than 2.85%.

3. Related theories

3.1. Theory and energy of heat generation

Microwave heating involves heat dissipation and microwaves propagation which causes the dipoles to vibrate and rotate. When the microwave energy emits from a microwave applicator (P_{in}) is irradiated inside the microwave applicator, the dielectric materials which has a dielectric loss factor absorbs the energy and are heated up. Then the internal heat generation takes place. The basic equation calculates the density of microwave power absorbed by dielectric material (P_1) is given by [14]:

$$P_1 = \omega \epsilon_0 \epsilon_r'' E^2 = 2\pi \cdot f \cdot \epsilon_0 \cdot \epsilon_r' (\tan \delta) E^2 \quad (2)$$

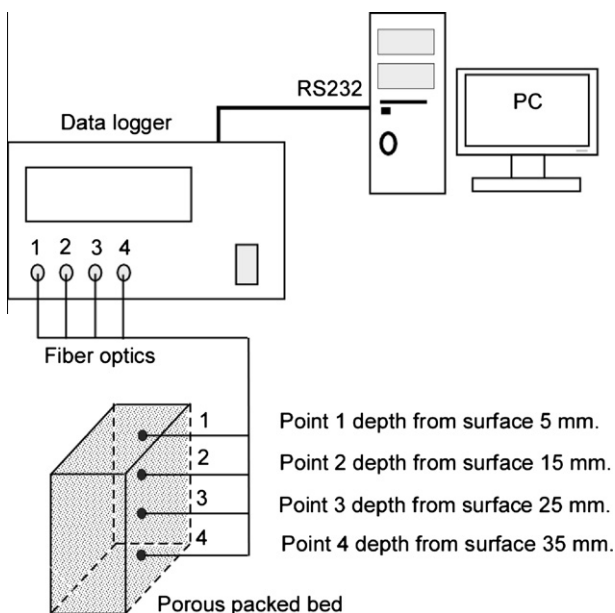


Fig. 2. Temperature measuring.

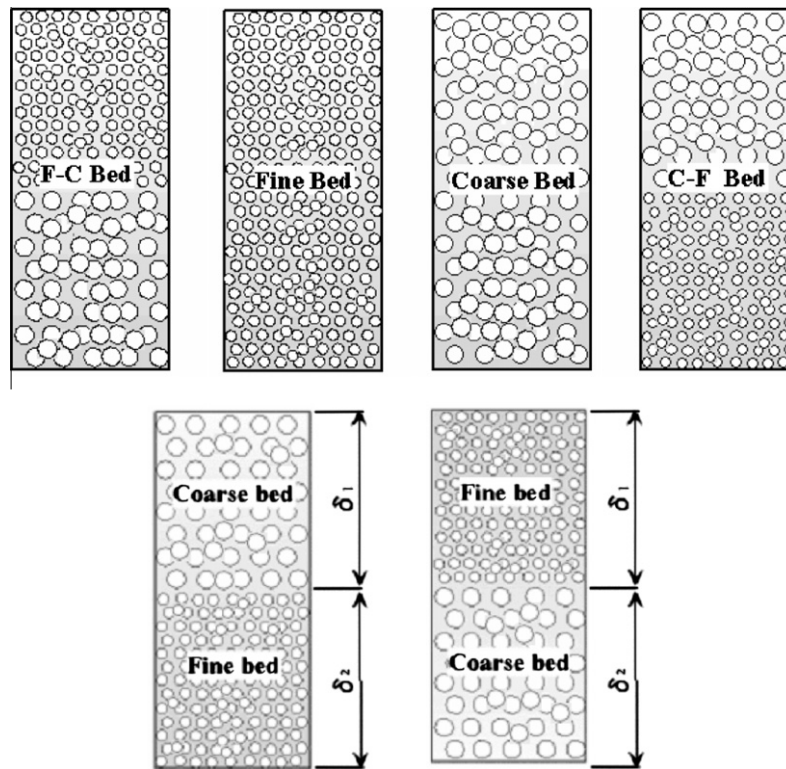


Fig. 3. Multi-layered porous packed bed (sample).

where E is electromagnetic field intensity; f is microwave frequency; ω is angular velocity of microwave; ϵ'_r is relative dielectric constant; ϵ_0 is dielectric constant of air and $\tan \delta$ is dielectric loss tangent coefficient.

From Eq. (2), P_1 is directly proportional to the frequency of the applied electric field and loss tangent coefficient and root-mean-square value of the electric field. It means that during an increasing of $\tan \delta$ of specimen, energy absorption and heat generation are also increased. While $\tan \delta$ is small, microwave will penetrate into specimen without heat generation. However, the temperature increase depends on other factors such as specific heat, size and characteristic of specimen.

When the material is heated unilaterally, it is found that as the dielectric constant and loss tangent coefficient vary, the penetration depth will be changed and the electric field within the dielectric material is altered. The penetration depth is used to denote the depth at which the power density has decreased to 37% of its initial value at the surface [16]:

$$D_p = \frac{1}{\frac{2\pi f}{v} \sqrt{\frac{\epsilon'_r \left(\sqrt{1 + \left(\frac{\epsilon''_r}{\epsilon'_r}\right)^2} - 1 \right)}{2}}} = \frac{1}{\frac{2\pi f}{v} \sqrt{\frac{\epsilon'_r (\sqrt{1 + (\tan \delta)^2} - 1)}{2}}} \quad (3)$$

where D_p is penetration depth ϵ''_r is relative dielectric loss factor and v is microwave speed. The penetration depth of the microwave power is calculated according to Eq. (3), which shows how it depends on the dielectric properties of the material. It is noted that products with huge dimensions and high loss factors, may occasionally be overheated to a considerably thick layer on the outer layer. To prevent such phenomenon, the power density must be chosen so that enough time is provided for the essential heat exchange between boundary and core. If the thickness of the material is less than the penetration depth, only a fraction of the supplied energy

will become absorbed. Furthermore, the dielectric properties of porous material specimens typically show moderate lossiness depending on the actual composition of the material. With large amount of moisture content, it reveals a greater potential for absorbing microwaves. For typical porous material specimens, a decrease in the moisture content typically decreases ϵ''_r , accompanied by a slight increment in D_p .

In the analysis, energy P_2 is required to heat up the dielectric material $W(g)$ which is placed in a microwave applicator. The temperature of material initially T_1 , is raised to T_2 . The energy P_2 can be estimated by the following calorific equation [17]:

$$P_2 = \frac{4.18 \cdot W \cdot C_p \cdot \Delta T}{t} \quad (4)$$

where W is weight of the dielectric material; C_p is specific heat of the dielectric material; ΔT is the increment of temperature ($T_2 - T_1$) and t is heating time.

Assuming an ideal condition, all of the oscillated microwave energy (P_{in}) is absorbed into the dielectric material; such internal heat generation as Eq. (2) shows takes place. In this case, the relation between P_{in} and P_2 is shown below:

$$P_{in} = P_2 \quad (5)$$

In a practical point of view, however, the transformation energy in applicator exists due to Eq. (2) the rate of microwave energy absorbed by means of the dielectric loss factor of the sample and Eq. (3) the energy loss in the microwave devices. Accordingly, by taking into account this transformation efficiency, the microwave oscillation output can be calculated by the following equations:

$$P_{in} = \frac{P_2}{\eta} \quad (6)$$

$$\eta = \frac{P_2}{P_{in}} \quad (7)$$

3.2. Incident, reflection, transmission and absorbed wave

In Fig. 4, microwave can be incidental into the packed bed, it can transmit through the packed bed, and it also can be reflected and absorbed by the porous packed bed. By power balance on control volume as shown in Fig. 4, the incident wave can be expressed as:

$$\begin{aligned} \text{Incident Wave (A)} &= \text{Reflected Wave (B)} \\ &+ \text{Transmitted Wave (C)} \\ &+ \text{Absorbed Wave (D)} \end{aligned} \quad (8)$$

where P_{in} is microwave power incident or microwave energy emitted from a microwave oscillator (Incident Wave (A)); P_{ref} is microwave power reflected (Reflected Wave (B)); P_{tran} is microwave power transmitted (Transmitted Wave (C)) and P_{abs} is microwave power absorbed (Absorbed Wave (D)).

In order to calculate the microwave power absorbed, Eq. (8) can be rearranged as:

$$P_{abs} = P_{in} - P_{tran} - P_{ref} \quad (9)$$

Next, refers to throughout this study, as shown in equations below:

$$P_{abs} = \dot{Q}_{abs} \quad (10)$$

The microwave power absorbed efficiency during microwave drying of the porous packed bed provides a true measure of the performance of the drying system which can be expressed as:

$$\eta_{abs} = \left[\frac{\text{Absorbed Wave (D)}}{\text{Incident Wave (A)}} \right] \times 100 \quad (11)$$

$$\eta_{abs} = \left[\frac{P_{abs}}{P_{in}} \right] \times 100 \quad (12)$$

$$\eta_{abs} = \left[\frac{\dot{Q}_{abs}}{P_{in}} \right] \times 100 \quad (13)$$

3.3. Mass and energy balance equation for the drying process

The conservation of mass for the control volume of drying porous packed bed is shown in Fig. 5. The mass balance equation can be written as [11]:

$$\frac{dm_{cv}}{dt} = \dot{m}_{g1} - \dot{m}_{g2} \quad (14)$$

Here, Eq. (14) is the mass flow rate balance for the control volume where \dot{m}_{g1} and \dot{m}_{g2} denote, respectively, the mass flow rate at inlet (1) and exit at (2). Similarly, a balance of water in air flowing through the porous packed bed leads to [11]:

$$W_d \frac{dM_p}{dt} = \dot{m}_a (X_1 - X_2) \quad (15)$$

where W_d is weight of dry material and M_p is particle moisture content, dry basis; this can be expressed as [11]:

$$M_p = \frac{W_b - W_d}{W_d} \quad (16)$$

where W_b is weight of material before drying; \dot{m}_a is the mass flow rate of dry air; X_1 and X_2 denote, respectively, absolute humidity of inlet and exit air. The left-hand side of the mass balance equation, Eq. (15), is the mass flow rate of water in the air flowing on porous packed bed surface, can be written as [11]:

$$\dot{m}_w = \dot{m}_a (X_2 - X_1) \quad (17)$$

In the drying processes, we apply the first law of thermodynamics (the law of conservation of energy) for the control volume

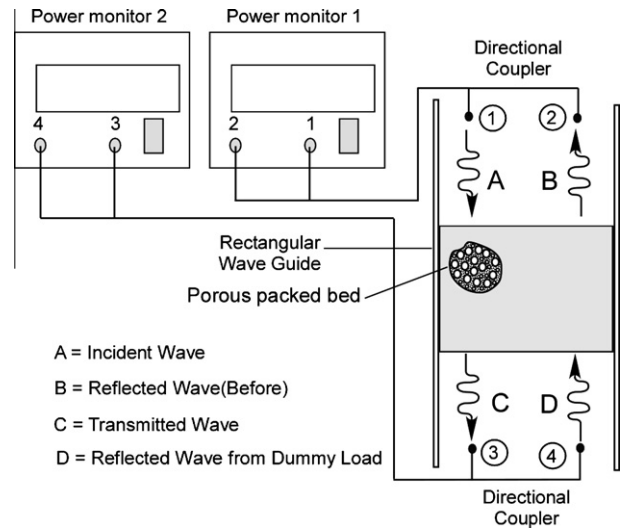


Fig. 4. Microwave power measuring.

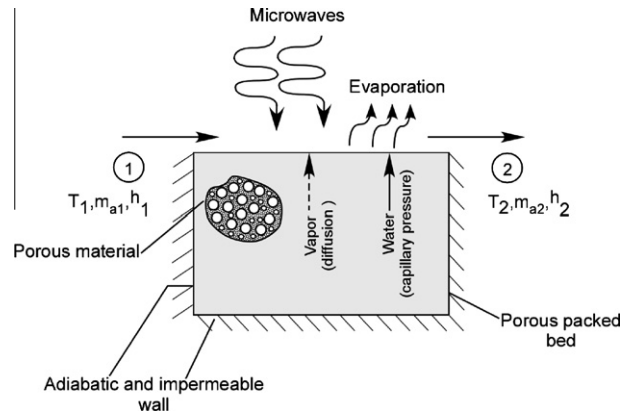


Fig. 5. Microwave and convective drying process.

shown in Fig. 5. The significant heat transfer is due to the heat of evaporation between the solid and the drying air, and there is also heat rejection to the surroundings. The energy rate balance is simplified by ignoring kinetic and potential energies. Since the mass flow rate of the dry air and the mass of dry material, within the control volume remain constant with time, the energy rate balance can be expressed as:

$$\frac{W_d(h_{m2} - h_{m1})}{\Delta t} = \dot{Q}_{evap} + \dot{m}_a(h_1 - h_2) + \dot{Q}_{abs} - \dot{Q}_{loss} \quad (18)$$

where \dot{Q}_{evap} is heat transfer rate due to water evaporation; \dot{Q}_{abs} is microwave energy required for heating up dielectric material; h_m is enthalpy of material; t is time; \dot{m}_a is mass flow rate of dry air; h is enthalpy of dry air and \dot{Q}_{loss} is heat transfer rate to the environment.

Assuming air as an ideal gas, thus the different in specific enthalpy are as follows [18]:

$$h_{m1} - h_o = c_m(T_{m1} - T_o) \quad (19)$$

$$h_{m2} - h_o = c_m(T_{m2} - T_o) \quad (20)$$

The enthalpy term of material in Eq. (18) can be written as [18]:

$$h_{m2} - h_{m1} = c_m(T_{m2} - T_{m1}) \quad (21)$$

where c_m represents the specific heat of the material. The enthalpy of moist air can be calculated by adding the contribution of each component as it exits in the mixture; thus the enthalpy of moist air is [18]:

$$h = h_a + Xh_v \quad (22)$$

The heat transfer rate due to phase change is [15]:

$$\dot{Q}_{evap} = \dot{m}_w h_{fg} \quad (23)$$

where h_{fg} is latent heat of vaporization.

3.4. Specific energy consumption and energy efficiency in drying process

The SEC was estimated in a combined convective - microwave drying processes. Considering the total energy supplied to dry porous packed bed from initial water saturation of 0.60 ($S_0 = 0.60$) to approximately a desired water saturation of 0.17 ($S_0 = 0.17$). The convective-microwave drying process was conducted in the same conditions with keeping the microwave power incident of 50 W, air temperature of 27.2 °C, and velocity of 3.71 m/s. The SEC is defined as follows:

$$SEC = \frac{\text{Total energy supplied in drying process}}{\text{Amount of water removed during drying}}, \frac{kJ}{kg} \quad (24)$$

$$SEC = \frac{(P_{in} + Q_{conv})\Delta t}{\text{Amount of water removed during drying}}, \frac{kJ}{kg} \quad (25)$$

where Q_{conv} is a convective heat transfer which can be calculated from [15]:

$$Q_{conv} = \bar{h}A(T_{surf} - T_{\infty}) \quad (26)$$

$$\bar{h} = \frac{\bar{N}_u k}{L} \quad (27)$$

where \bar{h} is convection heat transfer coefficient; A is porous packed bed surface area; T_{surf} is temperature at porous packed bed surface; T_{∞} is ambient temperature; \bar{N}_u is Nusselt number; k is thermal conductivity and L is length of surface of porous packed bed in direction of flow.

From Ref. [19], the energy efficiency for drying process is defined as:

$$\eta_e = \frac{W_d[h_{fg}(M_{p1} - M_{p2}) + c_m(T_{m2} - T_{m1})]}{\dot{m}_{da}(h_1 - h_0)\Delta t + \Delta t \dot{Q}_{abs}} \quad (28)$$

where c_m is material specific heat.

4. Results and discussion

The experiments of a combined of convective air and microwave drying process were conducted by varying layered configuration and layered thickness of porous packed bed. For porous packed beds of two different sizes (0.15 mm and 0.40 mm), microwave power incident of 50 W, air velocities of 3.71 m/s, and air temperature of 27.2 °C, the temperature distribution and the SEC were carried out.

4.1. Case I. Single layered porous packed bed (F, C bed)

Figs. 6 and 7 illustrate the distributions of temperature and averaged saturation of the F-bed and C-bed during the combined drying process, respectively. The thickness of packed bed is 50 mm ($d_p = 50$ mm). Temperature is measured at four positions of the sample. In Figs. 6 and 7 show the third position, which measured from surface downward to a depth of 25 mm. From

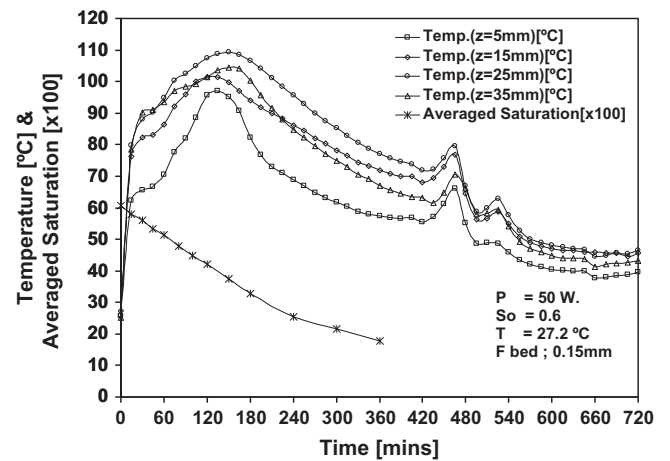


Fig. 6. Temperature and averaged saturation profiles with respect to elapsed time (F-bed, depth 50 mm).

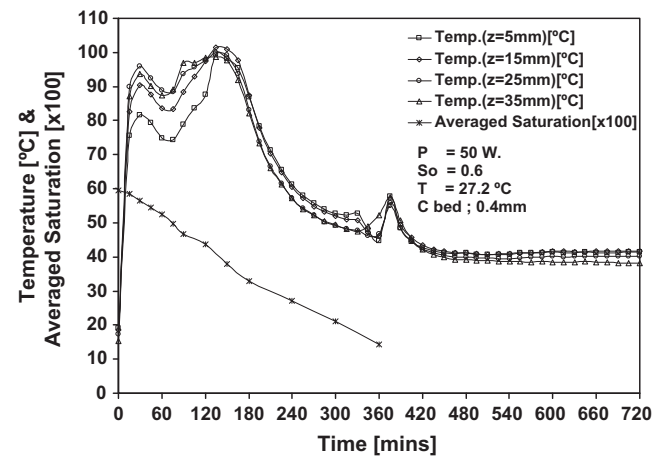


Fig. 7. Temperature and averaged saturation profiles with respect to elapsed time (C-bed, depth 50 mm).

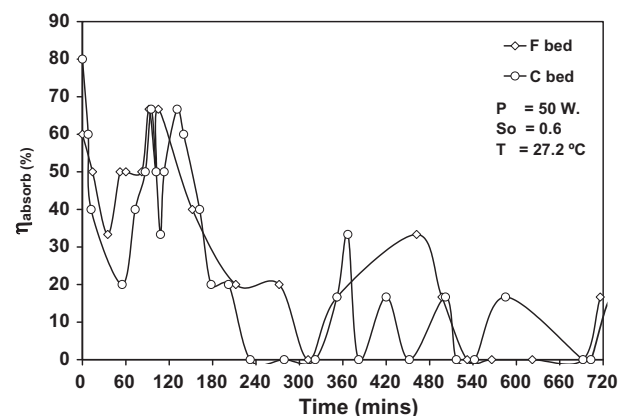


Fig. 8. The variation of microwave power absorbed efficiency with respect to elapsed time (F-bed, C-bed, depth 50 mm).

the starting time until 120 min elapsed, the microwave energy supplied is absorbed by porous packed bed sample, which is shown in Fig. 8 and whose microwave power absorbed efficiency can be calculated with Eq. (13). After that it is converted to heat the

sample temperature from ambient temperature to 109 °C and 95 °C for microwave power 50 Watts. At this point, there is high moisture content. The high moisture content at this period is reflected by the high loss tangent coefficient ($\tan \delta$). The next period from 120 to 720 min as shown in Fig. 8 depicts the increase transmitted wave and decrease reflected waves, which implies the microwave power absorption become lower than in the first period. Due to the fact that the moisture content is reduced, the loss tangent coefficient ($\tan \delta$) is decreased.

Figs. 6 and 7 show the temperature profiles measured by fiber-optic at various times and locations in the case of $S_0 = 0.6$, $d = 0.15$ mm and $d = 0.40$. The microwave and convective drying gives higher temperatures inside the drying sample while the surface temperature stays colder due to the cooling effect of surrounding air. At the same time the evaporation takes place at the surface of the sample at a lower temperature due to evaporative cooling. It is seen that the temperature profiles within the sample rise up steadily in the early stages of drying (about 60 min). Due to the large initial moisture content, the skin depth heating effect causes the majority of microwave to be reflected from the surface during early irradiation stage resulting in a lower rate of microwave power absorbed in the interior (Fig. 8). As the drying process proceeds (about 60–240 min), after the majority of moisture content is removed from the sample, the microwave can penetrate further into the sample as material dries (as referred to Fig. 8) where the strength of the microwave power absorbed increases (Fig. 8). During this stage of drying, the behavior of dielectric properties is influenced primarily by that of moisture content, and heating becomes more volumetric. In time about 240 min, the temperature starts to drop, this is mainly due to fact that the moisture inside the sample is significantly reduced, reducing dielectric loss factor as well as microwave power absorbed (Fig. 8). However, at long stages of drying (about 480 min: F-bed, 360 min: C-bed), the temperature increases rapidly due to the characteristic of dielectric loss factor, which becomes to dominant microwave drying at low moisture content where the stronger standing wave with a larger amplitude established within the sample. Nevertheless, near the end stages of drying as the majority of moisture content inside the sample is removed, this decreases the microwave power absorbed.

4.2. Case II. Two-layered porous packed bed

Experimental data of a combined drying process of two-layered porous packed bed are shown in Figs. 9–14, which corresponds to that of $S_0 = 0.60$ and $P_{in} = 50$ W. The data is along the center axis ($x = 55$ mm) of rectangular waveguide. Figs. 9 and 12 show the distribution of temperature and averaged saturation within F-C bed with layered thickness of fine bed as 10 and 25 mm, respectively. From a macroscopic point of view for the hydrodynamic characteristic properties within the two-layered porous packed bed, we will consider the liquid water transport at the interface between two beds where the difference of particle size is considered during microwave drying. As referred to Ratanadecho et al. [7], in the case of the same capillary pressure, a smaller particle size corresponds to higher water content. Now, consider the case where two particle sizes having same capillary pressure and different particle sizes at the interface are justified. The capillary pressure has the same value at the interface between two beds, but the water saturation becomes discontinuous at the interface of two beds. This is because of the differences of the water characteristics between the two beds, the liquid water will be moved from the coarse bed to the fine bed (which corresponds to a higher capillary pressure) resulting in a faster drying time.

On the other hand, in the case of C-F bed with layered thickness of coarse bed as 10 and 25 mm are shown in Figs. 10 and 13,

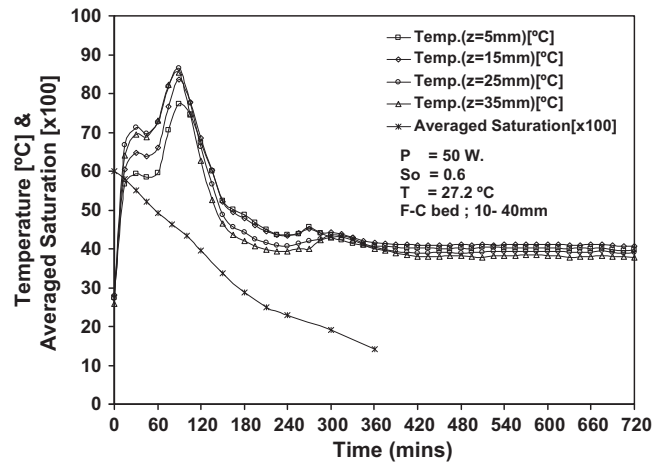


Fig. 9. Temperature and averaged saturation profiles with respect to elapsed time (F-C bed, depth 10–40 mm).

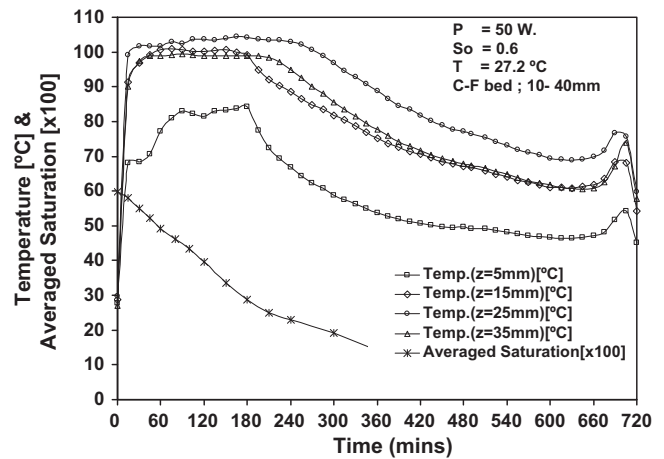


Fig. 10. Temperature and averaged saturation profiles with respect to elapsed time (C-F bed; depth 10–40 mm).

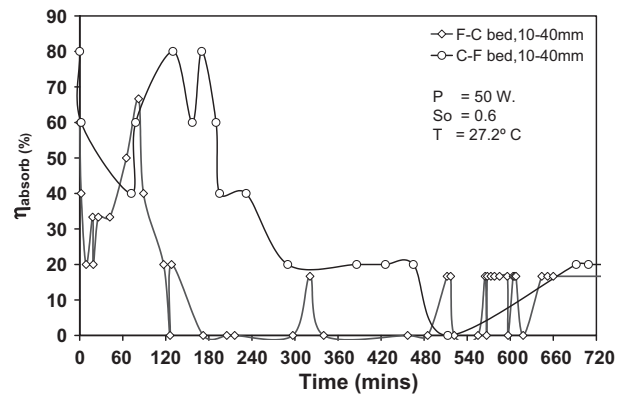


Fig. 11. The variation of microwave power absorbed efficiency with respect to elapsed time (F-C bed, C-F bed, depth 10–40 mm).

respectively. It is seen that the moisture content inside the fine bed is much higher because a coarse bed set on the fine bed retards the upward migration of liquid water at the interface between two beds, while the moisture content inside the coarse bed stays lower due to the lower capillary pressure [7].

The temperature profiles at various times and locations for both cases are shown in Figs. 10 and 13, respectively. Figs. 10 and 13 show that the temperature profile within the C–F bed rises up quickly in the early stages of drying process (about 10–60 min) However, its rise slows down after this stage. It is evident from the figure that near the end stages of drying as the moisture con-

tent inside the sample is reduced, the absorbed microwave power decreases (Figs. 11 and 14). Consequently, the temperature profiles are decreased in this stage of drying process. However, the temperature profile within the C–F bed (Figs. 10 and 13), corresponds to the moisture content profile where the temperature continuously rises faster than that in the case of F–C bed (Figs. 9 and 12). Further, the temperature remains high at the end of drying. This is because a stronger standing wave with a larger amplitude is formed inside the C–F bed and having of dry layer-coarse bed (upper layer) protects the reflection of wave from the surface, resulting in a higher rate of microwave power absorbed in the interior (Figs. 11 and 14).

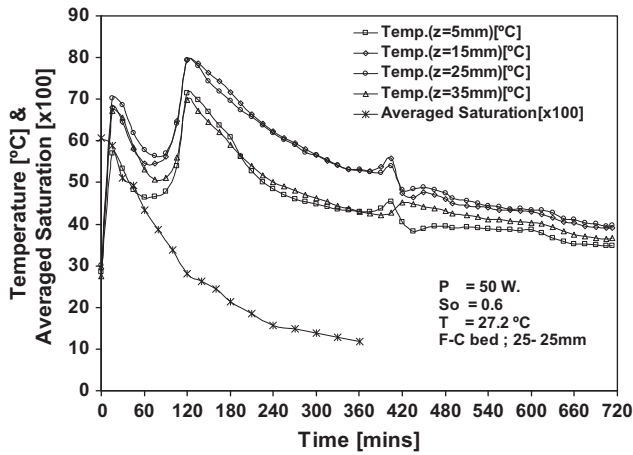


Fig. 12. Temperature and averaged saturation profiles with respect to elapsed time (F–C bed, depth 25–25 mm).

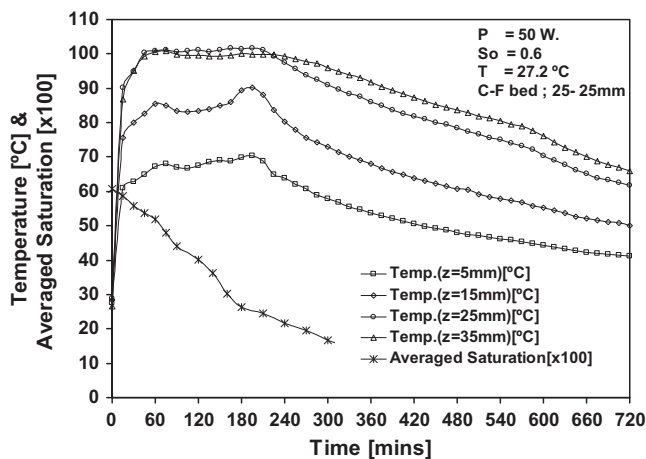


Fig. 13. Temperature and averaged saturation profiles with respect to elapsed time (C–F bed, depth 25–25 mm).

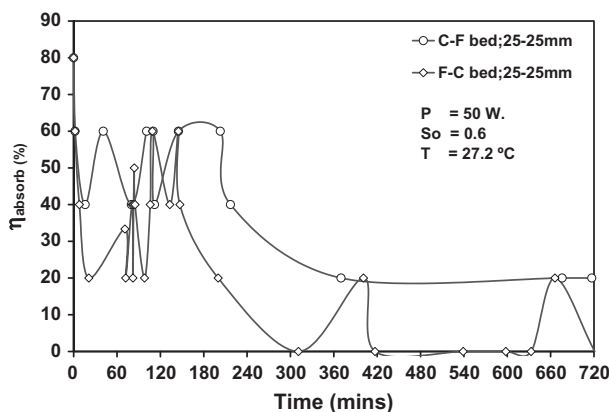


Fig. 14. The variation of microwave power absorbed efficiency with respect to elapsed time (F–C bed, C–F bed, depth 25–25 mm).

4.3. Specific energy consumption (SEC)

This subsection carried out the SEC of the porous packed bed with various layered configurations and layered thickness. The microwave power incident (P_{in}) is set at 50 W, air temperature of 27.2 °C with velocities of 3.71 m/s. The SEC within the various type of porous packed bed at drying time of 120, 240, and 360 min are shown in Figs. 15–17, respectively. From the Figs, it is shown that the SEC will increase with time proceed. This is because total energy supplied is remained while amount of water removed are decreasing during the drying process (ref. from Eq. (24)).

Comparing with the various packed bed configurations in Fig. 15, the SEC is lower corresponding to the case of F–C bed with each layered thickness of 25 mm. The SEC is 11.62 MJ/kg which means this packed bed type can remove higher amount of water than other types. After time proceed ($t = 240$ min) as seen in Fig. 16, For the case of F–C bed, it is interesting to observe that the value of the SEC is gradually decreased when the thickness of fine bead increases from 10 mm to 25 mm. After that, the SEC of the layer is gradually increased corresponds to increasing of fine bead thickness (30 mm to 40 mm). Finally, $t = 360$ min as seen in Fig. 17, the layered thickness of the packed bed was set to 10 and 25 mm with fine bead on top. It depicts that the specific energy consumption of the packed bed was lower than the coarse bead on top due to the capillary pressure [7] that cause moisture content to move to the surface quickly. In turn, these causes are force the moisture content to move out off the packed bed quickly, so the specific energy consumption is reduced, this effect to increase the efficiency of the system. Furthermore, it also observes that the relation between the SEC value and layered thickness of two-layered porous packed bed is non-linear. The reasons behind these phenomena need more investigations. Based on these studies, it is shown that the F–C bed with each layered thickness of 25 mm corresponds to the minimum value of SEC throughout drying process due to strongly capillary and osmotic action.

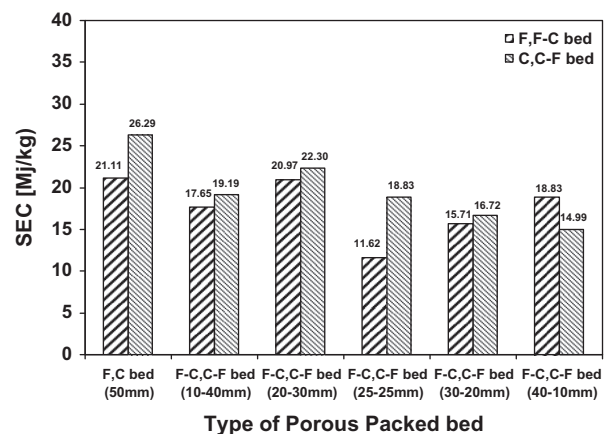


Fig. 15. Variation in specific energy consumption under microwave and convective drying at drying time 120 min.

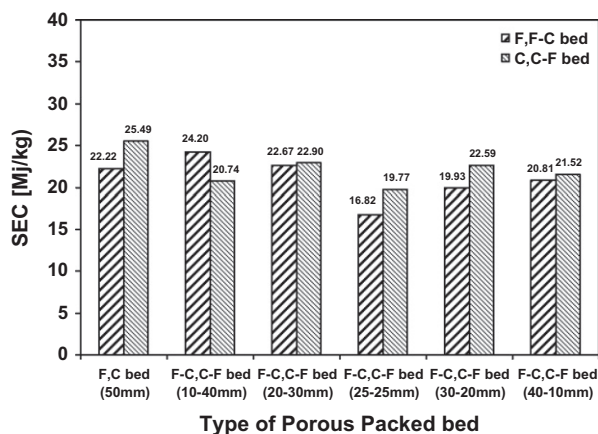


Fig. 16. Variation in specific energy consumption under microwave and convective drying at drying time 240 min.

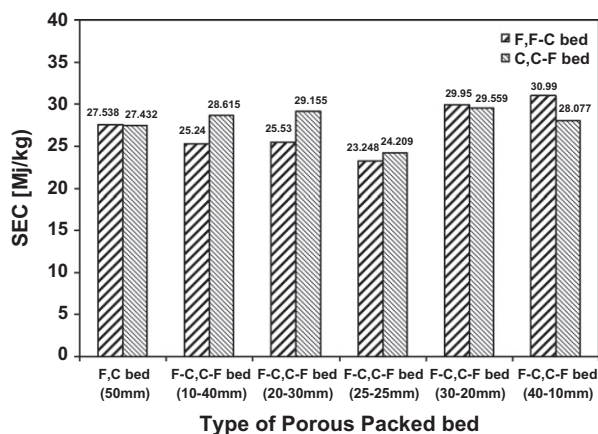


Fig. 17. Variation in specific energy consumption under microwave and convective drying at drying time 360 min.

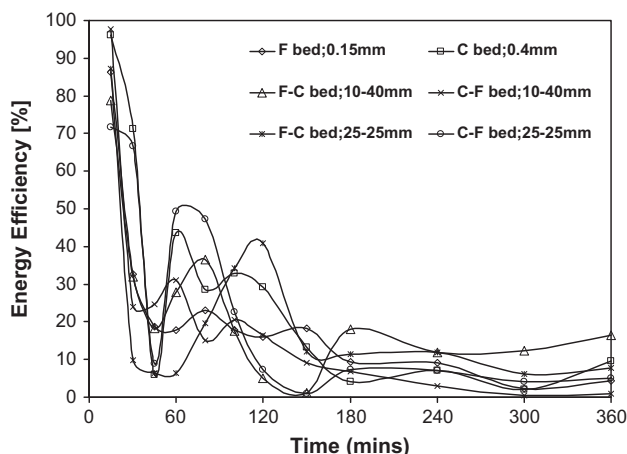


Fig. 18. Energy efficiency profiles with respect to elapsed time.

4.4. Energy efficiency

Fig. 18 shows the energy efficiency with respect to the drying time. It seems that the high energy efficiency near the starting period about 0–60 min due to the high quantity of moisture content in the packed bed, thus the wave absorption is more converted by

packed bed. The results are high energy efficiency after the vapor has moving from the surface of the porous packed bed. This causes the moisture content to quickly decrease and the low quantity of absorbed waves causes the decrease energy consumption and decrease microwave power absorbed efficiency (Eq. (13)). This cause is lower thermal efficiency; therefore, energy efficiency depends on the efficiency with which the waves are absorbed.

The energy efficiency profiles at various times and locations for six cases are shown in Fig. 18. The energy efficiency profile within the F–C and C–F bed rises up quickly in the early stages of drying process (about 10–120 min). However, its rise slows down after this stage (about 120–360 min). It is evident from the figure that near the end stages of drying as the moisture content inside the sample is reduced, this decreases the microwave power absorbed. Consequently, the energy efficiency profiles are decreased in this stage of drying process.

5. Conclusion

In this work, the energy efficiency and specific energy consumption of the combined convective–microwave drying process of multi-layered porous packed bed were presented in detail. Taking into considerations the results from these analyses, the following conclusion may be drawn on the SEC increased with decreasing energy efficiency during the drying process. Both the SEC and energy efficiency depend on the particle size in case of single-layered porous packed bed and layered configurations in case of two-layered porous packed bed.

The effects of layered configurations and layered thicknesses on the overall drying kinetics were clarified. The drying rate and energy efficiency in the case of the F–C bed with equal layered thickness of 25 mm is slightly higher than that other case of porous packed bed. It is also found that the drying rate relates to the moisture content within the packed bed.

This knowledge means that drying and heating processes using microwave energy can be designed to be significantly more efficient, reducing the drying period and so reducing specific energy consumption.

Acknowledgment

The authors are pleased to acknowledge the Thailand Research Fund (TRF) for supporting this research work.

References

- [1] Z.B. Maroulis, G.D. Saravacos, A.S. Mujumdar, Handbook of Industrial Drying, Taylor & Francis Group, Singapore, 2006.
- [2] N.V. Men'Shutina, M.G. Gordienko, A.A. Voinovskii, T. Kudra, Dynamics criteria for evaluating the energy consumption of drying equipment, Theor. Found. Chem. Eng. 39 (2003) 158–162.
- [3] E.K. Akpınar, Exergy and energy analysis of drying of red pepper slices in a convective type dryer, Int. Comm. Heat Mass Transfer 31 (2004) 1165–1176.
- [4] G.P. Sharma, S. Prasad, Specific energy consumption in microwave drying of garlic cloves, J. Food Eng. 31 (2005) 1921–1926.
- [5] J. Varith, P. Dijkanarukkul, A. Achariyaviriya, S. Achariyaviriya, Combined microwave-hot air drying of peeled longon, J. Food Eng. 31 (2007) 459–468.
- [6] S. Lakshmi, A. Chakkaravarthi, R. Subramanian, V. Singh, Energy consumption in microwave cooking of rice and its comparison with other domestic appliances, J. Food Eng. 78 (2005) 715–722.
- [7] P. Ratanadecho, K. Aoki, M. Akahori, Influence of irradiation time, particle sizes and initial moisture content during microwave drying of multi-layered capillary porous materials, ASME J. Heat Trans. 124 (2002) 151–161.
- [8] H. Feng, J. Tang, R.P. Cavaliere, O.A. Plumb, Heat and mass transport in microwave drying of porous materials in a spouted bed, A.I.Ch.E. J. 47 (2001) 1499–1512.
- [9] B. Abbasi Souraki, D. Mowla, Experimental and theoretical investigation of drying behaviour of garlic in an inert medium fluidized bed assisted by microwave, J. Food Eng. 88 (2007) 438–449.
- [10] H. Ogura, N. Hamaguchi, H. Kagea, A.S. Mujumdar, Energy and cost estimation for application of chemical heat pump dryer to industrial ceramics drying, J. Drying Technol. 22 (2004) 307–323.

- [11] S. Syahrul, F. Hamdullahpur, I. Dincer, Exergy analysis of fluidized bed drying of moist particles, *Int. J. Energy* 2 (2002) 87–98.
- [12] S. Syahrul, I. Dincer, F. Hamdullahpur, Thermodynamic modeling of fluidized bed drying of moist particles, *Int. J. Therm. Sci.* 42 (2003) 691–701.
- [13] S. Syahrul, F. Hamdullahpur, I. Dincer, Thermal analysis in fluidized bed drying of moist particles, *Int. J. Appl. Therm. Eng.* 22 (2002) 1763–1775.
- [14] P. Rattanadecho, The simulation of microwave heating of wood using a rectangular wave guide: influence of frequency and sample size, *Int. J. Chem. Eng. Sci.* 61 (2006) 4798–4811.
- [15] Frank P. Incropera, David P. Dewitt, Theodore L. Bergmann, Adrienne Lavine, *Fundamental of Heat and Mass Transfer*, John Wiley & Sons (Asia) Pvt., Ltd., Danvers, 2007.
- [16] W. Cha-um, P. Rattanadecho, W. Pakdee, Experimental analysis of microwave heating of dielectric materials using a rectangular wave guide (MODE: TE₁₀) (case study: water layer and saturated porous medium), *Int. J. Exp. Therm. Fluid Sci.* 33 (2009) 472–481.
- [17] S. Vongpradubchai, P. Rattanadecho, The microwave processing of wood using a continuous microwave belt drier, *Int. J. Chem. Eng. Process.* 33 (2009) 472–481.
- [18] Y.A. Cengel, M.A. Boles, *Thermodynamics: An Engineering Approach*, McGraw-Hill Companies, Inc., New York, 2002.
- [19] I. Dincer, M.A. Rosen, *Energy, Environment and Sustainable Development*, Elsevier Ltd., Burlington, 2002.